

Fractal analysis of the lunar free-air gravity field

Boyko Ranguelov¹, Rosen Iliev², Tzanko Tzankov³, Edelvays Spassov⁴

¹Department of Applied Geophysics, University of Mining and Geology "St. Ivan Rilski", Sofia, Bulgaria

^{2,3}Department of Geography, Ecology and Environment Protection, South-West University "Neofit Rilski", Blagoevgrad, Bulgaria

⁴Kinematics, Pasadena, CA, USA

Email addresses: branguelov@gmail.com¹, rosen_faust@abv.bg², tzankov1936@abv.bg³, espassov@hotmail.com⁴

Abstract

Recent dedicated lunar gravity mission- Gravity Recovery and Interior Laboratory (GRAIL) provided high-resolution gravity field data for the Moon. The collected data are the starting material for the construction of the latest gravity model GRGM1200A, up to a degree and order 1200° and with sensitivity down to <5 km resolution. This article presents the results of the study of the probable fractal structure of the lunar "free-air" gravity field, based on this data. The "free-air" gravity disturbances are the gravity perturbations computed at the reference radius of 1738 km. They show the gravity variations as measured by the spacecraft, and thus include contributions from both the surface topography and any sub-surface bodies. The results would throw a new light on the nature of the geophysical processes and phenomena that take place on the Moon.

Keywords: Moon, lunar, gravity field, anomalies, fractals

Introduction

The theory of fractals has been largely developed in the last few decades.. The results obtained are frequently used for explanation of the self-similarity and the self-organization of different elements related to the Earth and planetary science. The recent paradigm of the geodynamics has accepted the nonlinear behavior in time and space. For example, the fractal analysis is used in Plate tectonics elements [1], regional seismotectonic models [2], regional gravity field interpretation [3], seismicity time series [4]; [5]; [6]; [7]; [8]; [9]; [10]; [11]; [12], length of the coastlines [13], drainage network [14]; [15], global distribution of lakes [16], glacial landforms analysis [17] and many others.

In recent years, fractal analysis has become a major methodological tool for analyzing geological and geophysical processes and phenomena in other celestial bodies in the solar system. Fractal Theory has been successfully applied in the analysis of Mercury's asteroid craters [18], the gravitational fields and the topography of Mars ([19]; [20]) and Venus ([19]; [21]), topography of the Moon ([19]; [22]; [23]; [24]), lunar gravity anomalies over the basins of Lunar Farside [25].

The present study aims to analyze and interpret the probability of fractal structure of the "free-air" gravity anomalies within the Moon. Data from the latest lunar gravity model- GRGM1200A, to a degree and order 1200, with sensitivity down to <5 km resolution [26] is used.

Materials and Methods

Fractals analysis – methodological base

The classical example of a fractal object is defined by Mandelbrot [27]. If the length of an object P is related to the measuring unit length l by the formula:

$$P \sim l^{1-D} \tag{1}$$

then P is a fractal and D is a parameter defined as the fractal dimension. This definition was given by B. Mandelbrot in the early 60-s of the 20-th century. His ideas support the view that many objects in nature cannot be described by simple geometric forms, and linear dimensions, but they have different levels of geometric fragmentation. It is expressed into the irregularities of the different scales (sizes) – from very small to quite big ones. This makes the measuring unit extremely important parameter, because measuring of the length, the surface or the volume of irregular geometric bodies could be obtained so that the measured size could vary hundred to thousand orders. This fact was first determined when measuring the coastal line length of West England and this gave Mandelbrot the idea to define the concept of a fractal. In geology and geophysics is accepted that definition of the different “fractals” as real physical objects is most often connected to fragmentation [28]. This reveals that each measurable object has a length, surface or volume, which depends on the measuring unit and the object’s form (shape) irregularity. The smaller the measuring unit is, the bigger is the total value for the linear (surface, volume) dimension of the object and vice versa. The same is valid for 2D and 3D objects.

The theoretical approach for the linear case and for the 2D and 3D cases was developed by [29; 30]. They focused the attention on the relations between the smallest measuring unit and object’s size in analyzing linear (1D), 2D and 3D objects (Fig.2).

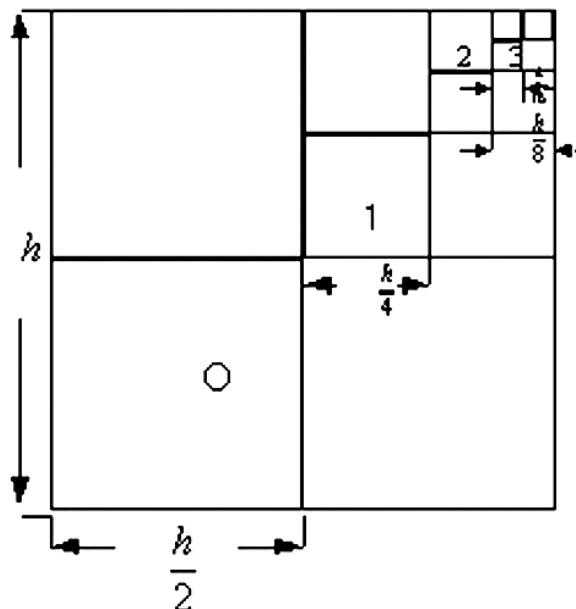


Fig.2: 2D fractal scheme – each linear element is 1/2 of the larger one.

If l is the measuring unit and with m we denote the obtained value for N at each measuring cycle, then the common sum of the lengths N at level m according to Turcotte [31] is:

$$N_m = (1 - p_c) \left(1 + \frac{n}{m} p_c + \left[\frac{n}{m} p_c \right]^2 \dots \left[\frac{n}{m} p_c \right]^m \right) \quad (2)$$

where p_c denotes the probability for measuring of each length for the corresponding cycle of the measurement.

Using formulas (1) and (2) we obtain the following formulas:

$$\frac{N_{m+1}}{N_m} = 2^D \quad (3)$$

for liner elements, and

$$\frac{N_{m+1}}{N_m} = (2^2)^D \quad (4)$$

for any area elements (surfaces).

Another definition of a fractal dimension is related to the serial number of measurement to each of the measuring units used and the object dimensions. If the number of the concrete measurement with a selected linear unit is bigger than r , then it might be presented by:

$$N \sim r^{-D} \quad (5)$$

and the fractal is completely determined by D as its characteristic fractal dimension.

The present study methodology, based on the correlation number-area, is following the algorithm presented and effectively applied in a number of previous works [32], [33], [2], [1], [34], [3].

The methodological approach follows the following steps:

- 1) Calculation of the number of the lunar "free-air" gravity anomalies (N) with corresponding area (in km^2) for the graphic. The objects are relatively round isometric positive and negative "free-air" gravity anomalies on the entire surface of the Moon, probably formed during the Moon history by the meteoritic impacts.
- 2) Presentation of the results in graphic form – on the X axis areas of the free-air gravity anomalies are plotted in logarithmic scale, and on the Y axis the corresponding numbers in linear scale are plotted.
- 3) The fractal dimensions (D) have been calculated using the data from the graphic and results discussed.

Data and Software

The analysis of the lunar "free-air" ("free-air" is the analog of the Earth's gravitometry terminology - as known on the Moon the air is missing) surface gravity anomalies was performed on the basis of GRID data (in GeoTIFF format) from the latest lunar gravity model GRGM1200A- Gravity Recovery and Interior Laboratory (GRAIL), to degree and order 1200, with sensitivity down to <5 km resolution [26]. The data have been explored using free Geographic Information System (GIS) QGIS. The study included the absolute values of the lunar free-air surface gravity field more than $+100$ and -100 mGals respectively. The aberration due to the Moon curvature is also considered.

Free-air gravity anomalies- reflection of the lunar elevation model and its elements

Free air gravity anomalies are considered as the best expressed relationship between the low depths gravitational bodies reflecting the gravity influence of the elevated structures (craters, hills, etc.) (Fig.2). By definition the free-air anomaly (frequently called Faye's anomaly) at the representative point is:

$$g_F = g_m - [g_0 - 0.3088(H+h)] = g_m + 0.3088(H+h) - g_0 \quad (6)$$

Where g_F is the free-air gravity anomaly, g_0 is the absolute gravity value at the point where the measured value is g_m . H is the height above average level and the h – is the level difference between the spheroid and the geoid ("Moonoid") at the same point. The values of the free-air anomalies calculated in this way reflect the gravity field originated from the lunar surface elevations (Fig.3).

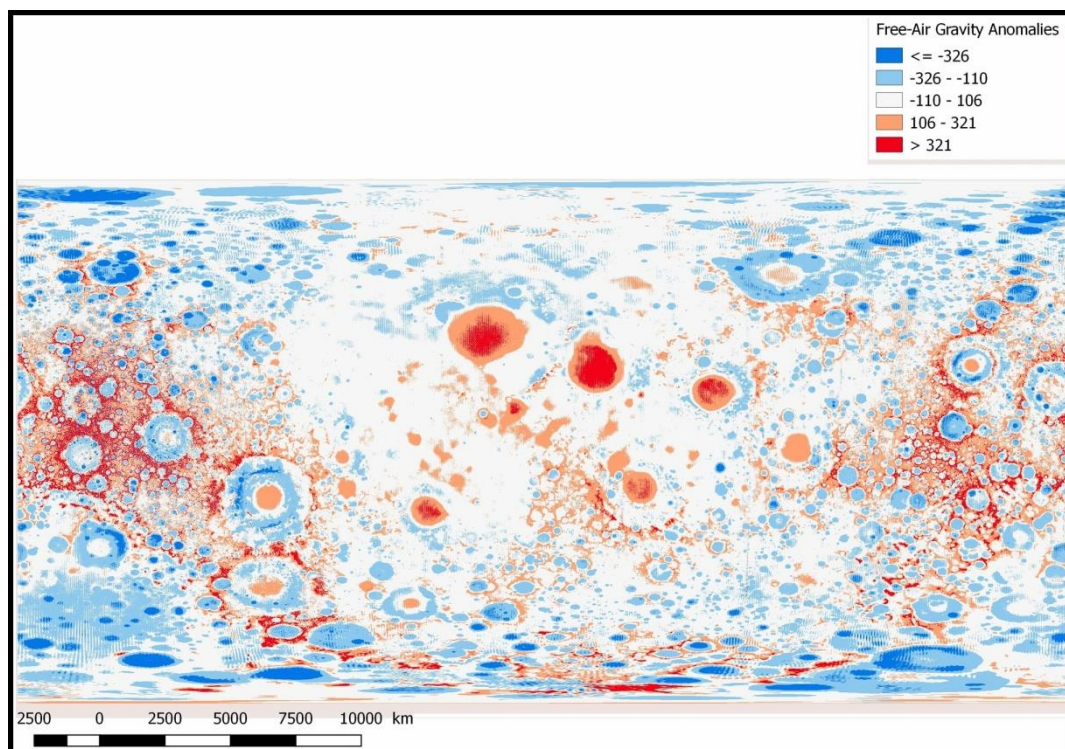


Fig.2: Distribution of the lunar free-air gravity anomalies (in mGals) (Data: Lunar Gravity Model GRGM1200A-Gravity Recovery and Interior Laboratory (GRAIL), [26])

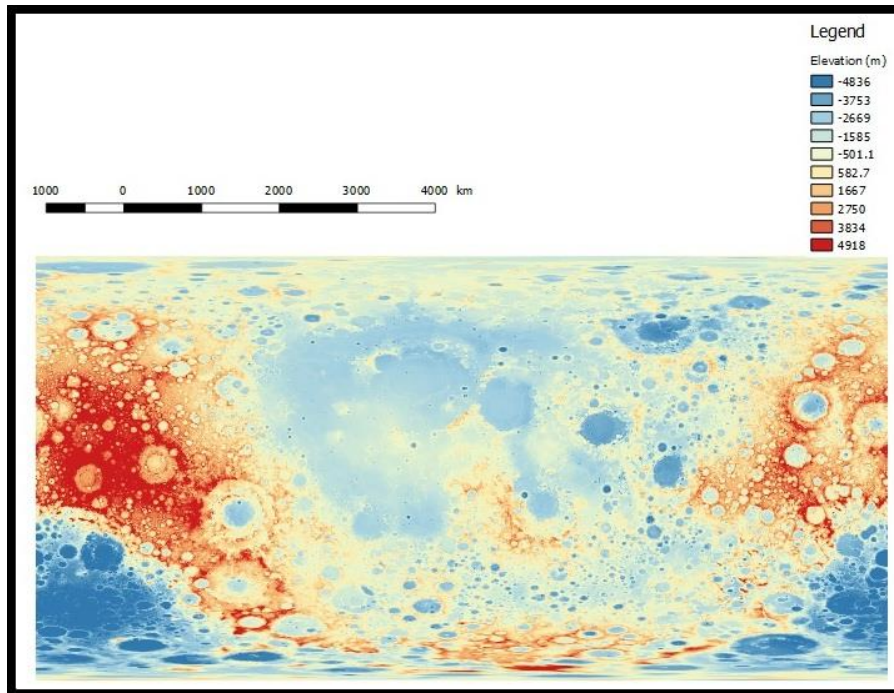


Fig.3: Moon topography map (DEM data: LOLA; [35])

Results and Discussion

The results of this study are graphically presented in Figure 4. The main conclusions and interpretations are discussed below.

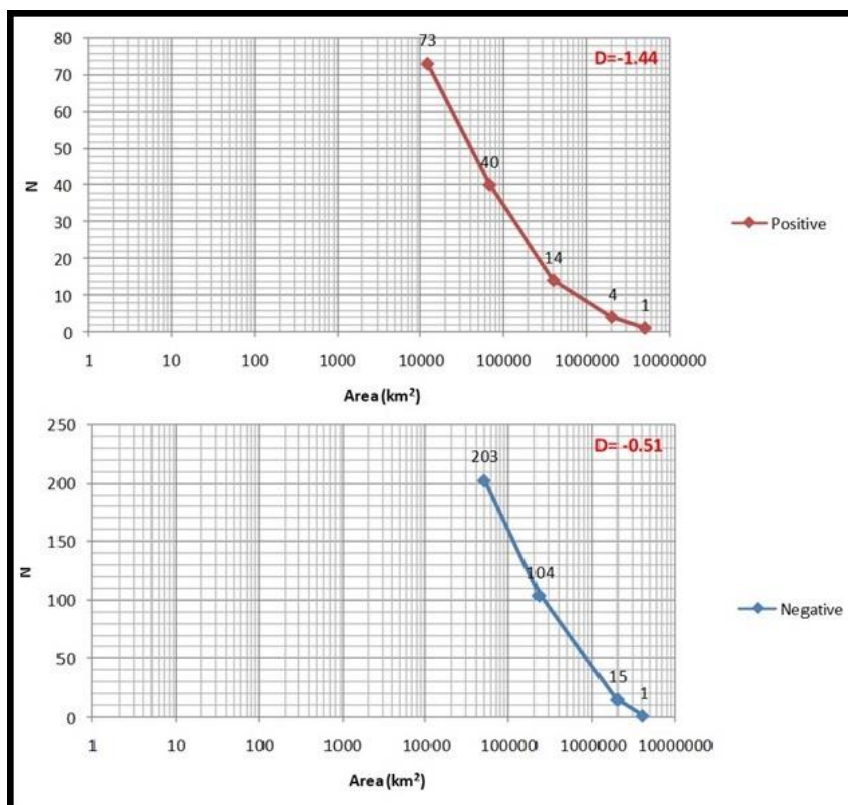


Fig.4: Fractal analysis of the lunar free-air gravity anomalies (Positive and Negative)

The normalized fractal dimensions, calculated in the Fig.4, are respectively $D=-1.44$ for the positive and $D=-0.51$ for the negative anomalies. The first value (-1.44) is approximately three times larger than -0.51. This means that the fractal distribution of the positive anomalies are much more nonlinear than the distribution of the negative ones (Fig.5). The negative anomalies are dominant and this is an interesting fact. This result could be explained by the use of a working hypothesis that the number of asteroids reached the lunar surface and generated the negative anomalies is larger than the number of asteroids generated the positive anomalies. If one is to go further in this direction, we can get an assumption that the asteroids with lower than average Moon density are three times more in numbers than the asteroids with higher density. The self-organized structure is visible even on the elevation map. When smaller asteroids impacted in the larger craters, they produced positive, as well as negative anomalies. This "spotted" structure is a confirmation that different in density asteroids created the lunar surface as well as the absolute free-air surface gravity anomalies.

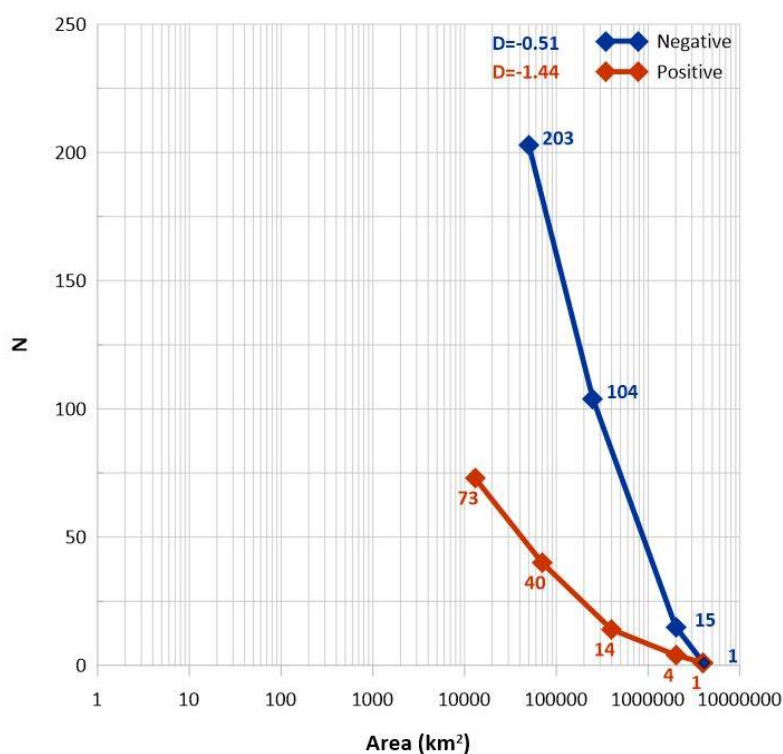


Fig.5: Fractal dimensions of the lunar free-air gravity anomalies (Positive and Negative) represented as surfaces

Conclusion

We use the classical fractal analyses of the free-air gravity anomalies measured and calculated on the entire Moon surface in this study. Both – positive and negative anomalies show clear fractal picture with the respective fractal dimensions $D(+)= -1.44$ and $D(-)= -0.51$. As it is considered that both sides (far and near to the Earth) are transformed and respectively shaped by the meteoritic impacts from most ancient geological times (even during the Moon's surface formation) up to the present days. It is clear that the negative anomalies are dominant due to the extrusion of Moon interior masses during the impact history and probably due to the lower density, asteroids impacted the Moon surface. The positive anomalies are most probably determined by the denser meteors. The fractal distribution with specific dimensions shows the self-similarity of the larger and smaller maskons of the Moon due to the impacts during the development phase of the Moon.

References

1. Ranguelov, B., Ivanov, Y. (2017) Fractal properties of the elements of Plate tectonics. Journal of mining and Geological Sciences. Vol. 60, Part 1, Geology and Geophysics, 83-89.

2. Ranguelov, B., Dimitrova, S., Gospodinov, D., Spassov, E., Lamykina, G., Papadimitriou, E., Karakostas, V. (2004) Fractal properties of the South Balkans seismotectonic model for seismic hazard assessment, Proceedings 5th Intl. Symposium on East Mediterranean Geology, Thessalonica, 643-646.
3. Tzankov, Tz., Iliev, R., Ranguelov, B. (2018) Fractal structure of the positive free-air gravity anomalies within the Balkan Peninsula. To Physics Journal. Vol.1, №3, Geology and Geophysics, 225-233.
4. Bak, P., Chen, K. (1995) Fractal dynamics of earthquakes. Fractals in the Earth Sciences, Plenum Press, New York, 227-235.
5. Bhattacharya, P., Chakrabarti, B.K., Kamal, Samanta, D. (2009) Fractal models of earthquake dynamics. Reviews of Nonlinear Dynamics and Complexity, ed. by H. G. Schuster, Wiley - VCH Verlag GmbH & Co. KGaA, 107 – 158.
6. Legrand, D. (2002) Fractal dimensions of small, intermediate and large earthquakes. Bulletin of the Seismological Society of America, Vol. 92, No. 8, 3318–3320.
7. Matsuzaki, M. (1994) Philosophical Transactions: Physical Sciences and Engineering. Vol. 348, No. 1688,, 449-457.
8. Mittag, R. (2003) Fractal analysis of earthquake swarms of Vogtland/NW-Bohemia intraplate seismicity. Journal of Geodynamics, 35, 1–2, 173-189. doi.org/10.1016/S0264-3707(02)00061-3
9. Öztürk, S. (2008) Statistical correlation between b-value and fractal dimension regarding Turkish epicentre distribution. Earth Sciences Research Journal, 16, 2, 103-108.
10. Pailoplee, S., Choowong, M. (2014) Earthquake frequency-magnitude distribution and fractal dimension in mainland Southeast Asia. Earth, Planets and Space, 6, 1-8. doi.org/10.1186/1880-5981-66-8
11. Srivardhan, V., Srinu, U. (2014) Potential of Fractal Analysis of Earthquakes through Wavelet Analysis and Determination of b Value as an Aftershock Precursor: A Case Study Using Earthquake Data between 2003 and 2011 in Turkey. Journal of Earthquakes, vol. 2014, 5 p. doi.org/10.1155/2014/123092.
12. Tosi, P., De Rubeis, V., Loreto, V., Pietronero, L. (2008) Space–time correlation of earthquakes. Geophysical Journal International, Vol. 173, Issue 3, 932–941; doi.org/10.1111/j.1365-246X.2008.03770.x
13. Mandelbrot, B.B. (1967) How long is the Coast of Britannia? Statistical self-similarity and fractional dimension. Science, 156, 636-638.
14. Burrough, P.A., (1981) Fractal dimension of landscapes and others environmental data. Nature, 294, 240-242.
15. Hastings, H.M., Sugihara, H. (1993) FRACTALS: A User's Guide for the Natural Sciences. Oxford Science Publications, 235 p.
16. Meybeck, M. (1995) Global distribution of lakes. In: Lerman, A., Imboden, D.M., Gat, J.R. (Eds.), Physics and Chemistry of Lakes, 2nd ed., Springer-Verlag, Berlin, 1–35.
17. Tzankov, Tz., Iliev, R., Mitkov, I., Stankova, Sv. (2018) About Fractal Geometry of the Glacial Cirques in Rila and Pirin Mountains (Southwest Bulgaria). Universal Journal of Geoscience, 6, 73-77. Doi: 10.13189/ujg.2018.060303.
18. Mancinelli, P., Pauselli, C., Perugini, D., Lupattelli, A., Federico, C. (2014) Fractal Dimension of Geologically Constrained Crater Populations of Mercury. Pure and Applied Geophysics, Springer Verlag, Volume 172, Issue 7, 1999–2008.
19. Turcotte, D. (1987) A fractal interpretation of topography and geoid spectra on the earth, moon, Venus, and Mars. Journal of Geophysical Research, vol. 92, 597-601.
20. Demin, S.A., Andreev, A.O., Demina, N.Y., Nefedyev, Y.A. (2017) The fractal analysis of the gravitational field and topography of the Mars. J. Phys.: Conf. Ser. 929 012002, 1-7. Doi :10.1088/1742-6596/929/1/012002

21. Demin, S.A., Andreev, A.O., Demina, N.Y., Nefedyev, Y.A. (2018) The fractal analysis of the topography and gravitational field of Venus. *J. Phys.: Conf. Ser.* 1038 012020, 1-6. Doi :10.1088/1742-6596/1038/1/012020
22. Nefedjev, A.Y. (2003) Lunar Surface Research Using Fractal Analysis. *The Journal of the Eurasian Astronomical Society*, Vol. 22, Issue 4-5, 631-632. Doi.org/10.1080/1055679031000139460
23. Baldassarri,A., Montuori,M., Prieto-Ballesteros,O., Manrubia, S.C. (2008) Fractal properties of isolines at varying altitude revealing different dominant geological processes on Earth. *J. Geophys. Res.*, 113, E09002, doi:10.1029/2007JE003066.
24. Huang, X, Jiang, X., Yu, T., Yin, H. (2009) Fractal-Based Lunar Terrain Surface Modeling for the Soft Landing Navigation. *Second International Conference on Intelligent Computation Technology and Automation*, Changsha, Hunan, China, 53-56. doi: 10.1109/ICICTA.2009.250
25. Kumar, A.V.S., Sekhar, R.P.R., Tiwari, R.M. (2016) Fractal Analysis of lunar Gravity anomalies over the Basins of Lunar Farside. *19th National Space Science Symposium (NSSS-2016)*, Poster Session, Kerala, India.
26. Goossens, S., Lemoine, F.G., Sabaka, T.J., Nicholas, J.B., Mazarico, E., Rowlands, D.D., Loomis, B.D., Chinn, D.S., Neumann, G.A., Smith, D.E., Zuber, M.T. (2016) A Global Degree and Order 1200 Model of the Lunar Gravity Field using GRAIL Mission Data. *47th Lunar and Planetary Science Conference*, Houston, TX, Abstract #1484.
27. Mandelbrot B. (1982) *The Fractal Geometry of Nature*. San Francisco: W.H. Freeman & Co., San Francisco, 68 p.
28. Korvin, G. (1992) *Fractal models in the Earth Sciences*. New York: Elsevier, 236 p.
29. Turcotte, D. (1986) Fractals and Fragmentation. *Journal of Geophysical Research*. 91, B2, 1921-1926.
30. Hirata T. (1989) Fractal dimension of fault system in Japan: Fractal structure in Rock geometry at various scales. *Pure and Applied Geophysics*, 131, 157-173.
31. Turcotte, D. (1986) A fractal model of crustal deformation. *Tectonophysics*, 132, 361-369.
32. Ranguelov, B., Dimitrova, S. (2002) Fractal model of the recent surface earth crust fragmentation in Bulgaria, *Comptes Rendus de l'Academy Sciences Bulgaria*. 55, 3, 25-28.
33. Ranguelov, B., Dimitrova, S., Gospodinov, D. (2003) Fractal configuration of the Balkan seismotectonic model for seismic hazard assessment, *Proceedings BPU-5, Vrnjacka Banja, Serbia and Montenegro*, 1377-1380.
34. Ranguelov, B. (2010) Nonlinearities and fractal properties of the European-Mediterranean seismotectonic model. *Geodynamics & Tectonophysics*, 1, 3, 225-230.
35. Smith, D.E., Zuber, M.T., Neumann, G.A., Mazarico, E., Head, J.W., III, Torrence, M.H. and the LOLA Science Team (2011) Results from the Lunar Orbiter Laser Altimeter (LOLA): global, high-resolution topographic mapping of the Moon, *Lunar Planetary Science Conference XLII*, Abstract 2350.